FORM 2

THE PATENTS ACT, 1970

(39 OF 1970)

&

The Patents Rules, 2003

COMPLETE SPECIFICATION

(Refer section 10 and rule 13)

TITLE OF THE INVENTION:

DECHLORINATION OF LINDANE AND ITS REMOVAL FROM WATER BY GRAPHENE NANOCOMPOSITES

---

2. APPLICANT:

(A) NAME: **INDIAN INSTITUTE OF TECHNOLOGY MADRAS**

(B) NATIONALITY: Indian

(C) ADDRESS: **INDIAN INSTITUTE OF TECHNOLOGY MADRAS**

　　　　　　IIT P.O

　　　　　　Chennai - 600 036

---

3. Preamble to the Description

COMPLETE SPECIFICATION

The following specification describes the invention

<div align="center">COMPLETE SPECIFICATION</div>

TITLE OF THE INVENTION

DECHLORINATION OF LINDANE AND ITS REMOVAL FROM WATER BY GRAPHENE NANOCOMPOSITES

FIELD OF THE INVENTION

The present invention relates to unusual degradation of the pesticide, lindane into isomers of trichlorobenzene and removal of the products from water by graphene nanocomposites.

BACKGROUND OF THE INVENTION

Graphene, [*Nat. Mater.* 2007, 6, 183] a 2D sheet of carbon atoms having two open faces is the basic structural unit of most other carbon allotropes such as graphite, carbon nanotubes and fullerenes. Since the discovery of graphene in 2004, [*Science* 2004, 306, 666.] it is investigated for diverse physical and chemical applications. To mention a few are, thermal conductivity due to phonon transport, [*J. Appl. Phys.* 2011, 110, 084302] high electrical conductivity due to Dirac transport, [*Nature* 2005, 438, 197] enhanced photoconductivity, [*Nanoscale* 2013, 5, 381] anomalous quantum hall effect, [*Nat. Mater.* 2007, 6, 183] electronic properties, [*Science* 2004, 306, 666] drug delivery, [*Adv. Drug Delivery Rev.* 2011, 63, 1352] electrochemical and solid-state gas sensors, [*Biosens. Bioelectron.* 2011, 26, 4637-11; *Chem. Soc. Rev.* 2012, 41, 2283; *Environ. Sci. Technol.* 2010, 44, 1167; *Adv. Funct. Mater.* 2012, 22, 1981; *Adv. Funct. Mater.* 2010, 20, 3117] hydrogen storage, [*ACS Nano*, 2009, 3, 2995; *Energy Environ. Sci.* 2011, 4, 668; *Energy Environ. Sci.* 2011, 4, 1113] and catalysis. [*ChemCatChem* 2012, 4, 2026; *Nat. Commun.* 2012, 3; *J. Am. Chem.Soc.* 2009, 131, 8262] However, its application in molecular adsorption and hence, in water purification [*J. Hazard. Mater.* 2011,186, 921; *J. Hazard. Mater.* 2013, 246–247, 213; *ACS Appl. Mater. Interfaces* 2011, 3, 1821; *Journal of Hazardous Materials* 2011, 192, 1515; *Environ. Sci. Technol.* 2012, 46, 977; *Appl. Surf. Sci.* 2013, 264, 329] has gained momentum only recently. Special properties like large surface area, [*Adv. Mater.* 2010, 22, 3906] antibacterial nature, [*ACS Appl. Mater. Interfaces* 2011, 3, 2643; *ACS Nano* 2011, 5, 6971; *ACS*

<div align="center">2</div>

Nano 2010, 4, 4317; *Environ. Sci. Technol.* 2013, 47, 8724] reduced cytotoxicity [*Toxicol. Lett.* 2011, 200, 201; *ACS Nano* 2010, 4, 5731] and tunable chemical properties made this material attractive for the application. Overwhelming number of articles published recently reporting the ability of graphene to purify water, support this claim. [*ACS Nano* 2010, 4, 3979-44; *ACS Appl. Mater. Interfaces* 2012, 5, 425; *ACS Appl. Mater. Interfaces* 2012, 4, 4156; *Environ. Sci. Technol.* 2010, 44, 8692; *Colloids Surf.*, B. 2012, 90, 197; *Int. J. Mod. Phys. B* 2012, 26; *J. Hazard. Mater.* 2012, 205-206, 229; *Nano Lett.* 2012, 12, 3602; *Small* 2013, 9, 273; *J. Hazard. Mater.* 2012, 215-216, 272; *Nanoscale* 2013, 5, 3149; *Adv. Funct. Mater.* 2013].

On the other hand, there are prior arts existing related to the removal of lindane/pesticide from water using reduced graphene oxide with silver nanoparticles by adsorption, PCT Publication No. WO 2012/142025, WO 2012/170086 and PCT/IB2011/002740. However, to the best of our knowledge, chemical reactions on graphene or graphene nanocomposites and detailed mechanisms of adsorption of organic molecules on graphene remain unexplored.

SUMMARY OF THE INVENTION

The present invention relates to unusual degradation/dechlorination of the lindane pesticide into trichlorobenzene isomers and its removal from water by graphene composites.

The said conversion comprise,

(i) Degradation of lindane to different isomers of trichlorobenzenes (TCBs) and

(ii) Adsorption of the degraded products on RGO

Wherein, the conversion of lindane ($C_6H_6Cl_6$), a persistent organochlorine pesticide to different isomers of trichlorobenzenes (TCBs, $C_6H_3Cl_3$) is carried over the silver nanoparticles (Ag NPs) supported on RGO and TCB's were adsorbed on graphene sheet by π-π interactions and degraded.

BRIEF DESCRIPTION OF THE DRAWINGS:

Fig. 1 shows TEM image of RGO@Ag composite, the scale bar shows the size distribution of the Ag NPs (5 nm). Inset shows UV/Vis spectrum of RGO (blue trace) and RGO@Ag (red trace). The photograph shows the dispersed nature of RGO@Ag.

Fig. 2 shows A) IR spectrum of lindane (red trace) and the product (blue trace), B) UV/Vis spectrum of (a) lindane and the (b) product, inset showing the photograph before and after reaction, C) TEM image of RGO@Ag after reaction and D) HRTEM-EDAX of the composite after reaction along with the elemental mapping which confirms the presence of silver and chlorine on the surface.

Fig. 3 shows mass spectrum of (A) lindane (red trace) and the (B) product (blue trace). Inset shows the isotopic distribution of chlorine and the corresponding molecular structure of the analytes.

Fig. 4 shows MS-MS of the peaks at m/z 179, 181 and 183 (a, b and c, respectively). The chemical structure of the peak m/z 180, 163 and 150 are shown in the inset. The various isotopologue ions and their fragments are labeled. The ions may have isomeric structures.

Fig. 5 shows ^{1}H NMR of A) lindane and B) the degraded product. The insets show the Raman spectra of a) lindane and b) the product. The schematic in A is the structure of lindane and the products. i) Optical image of the crystals of TCBs.

Fig. 6 shows Figure 6: A) GC-ECD traces and B) UV/Vis data showing the degradation of lindane and removal of the degraded product from the solution with respect to time. The dotted areas in A correspond to lindane and TCBs. As can be seen, the lindane peak at 0 min decreases with time. The TCBs peaks increases and then decreases due to its removal by the composite. In B, the lindane intensity continuously decreases.

Fig. 7 shows schematic showing the mechanism of adsorption of lindane on graphene substrate (not to scale).

Fig. 8 shows effect of A) concentration and B) initial pH on the removal efficiency of lindane using RGO@Ag.

Fig. S1 shows HRTEM image of RGO. Nanometer thick folding of the sheets can be seen. Scale bar is 200 nm.

Fig. S2 shows HRTEM image of GRP@Ag with varying silver ion concentration A) 0.01, B) 0.05 and C) 0.1

mM, respectively. D) HRTEM-EDAX spectrum of GRP@Ag.

Fig. S3 shows a) SEM image of a RGO@Ag after reaction. b & c) Elemental mapping of image a showing the presence of silver and chlorine, respectively. SEM-EDAX of the image a. The scale bar is the same in a, b and c.

Fig. S4 shows GC-ECD data of lindane (light blue trace) and the degraded product (black trace) after 5 min of reaction (note that in this case lindane was initially dissolved in hexane and spiked). The dotted box corresponds to the peak of lindane

Fig. S5 shows GC-MS spectrum of A) lindane and B) the degraded product.

Fig. S6 shows MS^2 of the peak of the degraded product trichlorobenzenes (m/z 180) at collision energy 60.

Please note that there are isomeric structures of the TCBs, only one isomer is shown here

Fig. S7 shows Raman spectrum of the product trichlorobenzenes, showing luminescence background.

Fig. S8 shows UV/Vis spectrum of silver nanoparticle and the inset shows their HRTEM image.

Fig. S9 shows UV/Vis spectrum showing the negligible removal/degradation capacity of lindane when treated with A) silver nanoparticles and B) graphene. The inset in figure B shows the HRTEM image of graphene.

Fig. S10 shows UV/Vis spectrum showing the comparison of the removal capacity of lindane using the composite and elemental silver.

Fig. S11 shows enlarged picture of GC-ECD after 2 min of reaction (with lindane and GRP@Ag) showing the presence of both lindane peak and the intermediate (trichlorobenzenes).

Fig. S12 shows UV/Vis spectrum showing the dependence of silver nanoparticle concentration towards the degradation of lindane.

Fig. S13 shows effect of A) tap water and B)100 ppm of NaCl solution on the removal efficiency of lindane using RGO@Ag.

Referring to the drawings, the embodiments of the present invention are further described. The figures are not necessarily drawn to scale, and in some instances the drawings have been exaggerated or simplified for illustrative purposes only. One of ordinary skill in the art may appreciate the many possible applications and variations of the present invention based on the following examples of possible embodiments of the present invention.

DETAILED DESCRIPTION OF THE INVENTION

The present invention relates to degradation / dechlorination of the lindane pesticide into trichlorobenzene isomers and its removal from water by graphene composites.

The said conversion comprise of,

    (i) Degradation of lindane to different isomers of trichlorobenzenes (TCBs) and

    (ii) Adsorption of the degraded products on RGO

Wherein, the conversion of lindane ($C_6H_6Cl_6$), a persistent organochlorine pesticide to different isomers of trichlorobenzenes (TCBs, $C_6H_3Cl_3$) is carried over the silver nanoparticles (Ag NPs) supported on RGO and TCB's were adsorbed on graphene sheet by π-π interactions and degraded.

The said reaction is unique to the composite and does not occur on RGO and nanoparticles of Ag separately. The products of the reaction are extensively characterized using spectroscopic techniques such as GC-MS, ESI-MS, IR and NMR, which unequivocally confirm their identity. The as-formed TCBs were removed from the aqueous medium by adsorption on the same composite. Adsorption is physical in nature, but mediated through strong π-π interactions. The study reveals the unusual chemical reactivity of graphene-metal composites and their potential for water treatment.

The invention demonstrates the chemical reactivity of graphene-silver nanocomposites(RGO@Ag), specifically, the degradation of lindane by silver nanoparticles (Ag NPs) supported on RGO and the adsorption of the degraded products on RGO. Lindane was used as a model system considering its persistent nature and difficulty in removal by conventional methods. Lindane, being neurotoxic, affects kidney, liver and the nervous system and is also a potent carcinogen.[*Chemosphere* 1999, 39, 1249; *Psychosomatics* 1999, 40, 513; *Environ. Pollut.* 1998, 103, 193]. Recent reports from India and other parts of the world indicate that lindane is widely present in surface and groundwater sources. [*Hazard. Mater.* 2010, 175, 680; *Chem. Eng. J.* 2010, 161, 83] Thus, there is an urgent need to find new and effective solutions to remove persistent organic pollutants like lindane from the contaminated environment.[*Springer Netherlands*, 2009, 151] The reaction reported here will provide a new methodology for decontaminating groundwater.

EXPERIMENT

    Materials: Natural graphite flakes were procured from Active Carbon India Pvt. Ltd. Sulfuric acid (H_2SO_4, 95-98%), ammonia (NH_3, 30%), and hydrochloric acid (HCl, 36%), were

purchased from Rankem Chemicals Pvt. Ltd., India. Hydrazinemonohydrate (N>99%), Phosphorus pentoxide (P$_2$O$_5$, 95 %), and hydrogen peroxide (H$_2$O$_2$purchased from SD Fine Chemicals Pvt. Ltd., India. Potassium peroxydisulfate (K$_2$ was purchased from Sisco Research Laboratories Pvt. Ltd., India. Potassium permanganate (KMNO$_4$, 98.5 %) was purchased from Merck, India. Lindane (HPLC assay 95 %) was purchased from Sigma Aldrich. Two separate 1000 mg/L of lindane stock solutions were prepared by dissolving the required quantity of lindane in pure ethanol (99.9%) and n-hexane (99.9%) and kept under refrigerated condition. Working concentrations of lindane were prepared from the stock solutions by dilution using deionized water (DW). All chemicals were of analytical grade and used as received, without any further purification. *Synthesis of RGO@Ag:* A procedure similar to Modified Hummers [*J. Am. Chem. Soc.* 1958, 80, 1339, 58; *Chem. Mater.* 1999, 11, 771] method was used to synthesize graphene oxide (GO) from graphite powder. The reduction of GO to RGO was done through the chemical route as reported by Li et al. [*J. Hazard. Mater.* 2011, 186, 921., *Nat. Nanotechnol.* 2008, 3, 101.]. Working concentrations of RGO was prepared by appropriate dilution of 0.01 wt%, stock RGO dispersion. For making RGO@Ag, 25 mL of RGO was taken and calculated amount of AgNO$_3$ was added to it, such that the final concentration of the composite was 0.01, 0.05 and 0.1 mM, respectively. This solution was kept undisturbed for 24 h at room temperature (30 ± 2°C), which allows the formation of Ag NPs over graphene. The composite was dialysed using distilled water to remove unwanted ions and was stored in glass bottles for further use. RGO@Ag (0.01 wt% of RGO and 0.01 mM AgNO was used for all experiments unless otherwise mentioned.

Adsorption Experiments: All adsorption studies were done in 20 mL batch reactors at room temperature (30 ± 2°C) keeping 5 mL as the working volume. Required volume of lindane stock solution was spiked to the RGO dispersion to get the working concentration. Please note that the working solution contained a small amount (<0.5% by volume) of ethanol or hexane which originated from the lindane stock solution. The solutions were kept for stirring for a predetermined time interval and the liquid was separated from the dispersion using a 200 nm membrane filter paper. The filtrate, extracted with hexane, was analyzed for residual lindane and degradation products using gas chromatography (GC) (PerkinElmer, Clarrus 680) equipped with electron capture detector (ECD). The analysis condition was programmed as following; run time,

7

38.5 min; injector temperature, 200°C; injection rate, 12.5 pts/s and carrier gas flow rate, 1 mL/min and the products were detected using ECD (hexane was used as the solvent for all GC-ECD characterization). The effect of contact time, pH and RGO@Ag dose on removal of pollutant was evaluated by varying the parameters in the appropriate window. All experiments except kinetics studies were conducted by batch equilibration method. To test interference of other ions in degradation of lindane and then removal of the degraded products, studies were conducted also by spiking required concentration of lindane in tap water (TW). All the experiments were conducted in duplicate, with proper control and the samples were analyzed immediately.

Instrumentation: UV/Vis spectrum was measured using a Perkin-Elmer Lambda 25 UV/Vis spectrophotometer. Raman spectra of GO and RGO were collected using a confocal Raman spectrometer (WiTec GmbH CRM 200). RGO and RGO@Ag samples were imaged using a high-resolution transmission electron microscope (HRTEM) with a UHR polepiece (JEOL 3011, 300 kV) equipped with analyzer foer energy dispersive analysis of X-rays (EDAX) (Oxford). Scanning electron microscopy (SEM) equipped with EDAX (FEI Quanta 200, Czechoslovakia) was also used to record the surface morphology, elemental composition and elemental map of the samples. FTIR spectrum was recorded on Nicolet 6700 spectrometer. Residual concentrations of lindane in water samples were analyzed using GC-ECD. The mass spectrometric studies were done using an electrospray system, 3200 Q-TRAP LC/MS/MS (Applied Biosystems).

RESULTS AND CONCLUSION

Graphene prepared in the solution phase (RGO) showed a characteristic UV/Vis peak centered at 271 nm (blue trace in Figure 1). As RGO characterization is reported extensively, [*J. Hazard. Mater.* 2011, 186, 921., 25, 36; *ACS Appl. Mater. Interfaces* 2011, 3, 2643, *Int. J. Mod. Phys. B* 2012, 26] we do not discuss this here in detail. RGO@Ag composite was formed through an oxidation-reduction process, in which RGO gets oxidized and silver gets reduced to silver nanoparticle and anchored onto the RGO surface. The recorded UV/Vis spectrum of RGO@Ag showed the peak corresponding to RGO (269 nm) and an additional plasmonic peak centered around 420 nm indicating the formation of Ag NPs (red trace in Figure 1) on the RGO surface. The small blue shift (2 nm) observed in the peak position of the parent RGO can be

ascribed to its partial oxidation. Figure 1 shows the HRTEM image of RGO@Ag (silver ion concentration 0.01 mM), the corresponding image for parent RGO is given in SI Figure S1. The graphene sheets with characteristic wrinkles are clearly visible (marked in the figure) in the image. The sheets are measured to be micrometer in size and the edges and wrinkles are 1.0–1.5 nm thick, which indicates graphene sheets with bi-layer thickness. The black dots seen in HRTEM image are due to the presence of Ag NPs over graphene sheets. The well-dispersed particles are almost of uniform size (approx. 5 nm) and spherical in shape. The sizes of the Ag NPs formed are found to be a function of concentration of the silver precursor added initially. Increase in precursor concentration from 0.01 to 0.1 mM of $AgNO_3$ resulted in the formation of particles of size varying from 5 to 50 nm (detailed discussion is in SI S2). The graphenic nature of the sheet is intact even after the formation of the composite. The presence of Ag peak in HRTEM-EDAX spectrum of the composite further confirms the deposition of silver on the RGO sheets (Figure S2D).

Pristine graphene is hydrophobic in nature, but the carboxylic group [*ChemPhysChem* 2010, 11, 2131, *Nano Lett.* 2008, 8, 1679] present in RGO is hydrophilic, which helps in forming a stable dispersion in water. The reduction of silver to Ag NPs by graphene does not affect the stability of the dispersion. This is evident from the photograph shown in the inset of the Figure 1. When a non-polar solvent like toluene or hexane is added to RGO dispersed in water, the RGO sheets prefer to stay at the interface and can act as an interfacial catalyst or reactant. When lindane dissolved in hexane was spiked into the graphene dispersion (0.01 wt%), the graphene sheets interacted with hexane and lost its dispersibility as shown in the inset of Figure 2B. The Ag NPs in the composite (RGO@Ag) react with lindane forming a degradation product.

Extensive characterizations with various spectroscopic and microscopic techniques were performed to establish the degradation products; a brief summary of these data is presented below. The FT-IR spectrum of lindane in Figure 2A (red trace) shows a prominent peak at 725 cm^{-1} due to C-Cl stretching and at 1386 and 1459 cm^{-1} due to bending vibrations of six C-H groups. The IR spectrum of the product after reacting with RGO@Ag is recorded (Figure 2A (blue trace)). The evolution of new peaks around 887, 1067 and 1139 cm^{-1} are due to the bending vibrations of =C-H group and the weak peak at 3189 cm^{-1} is due to aromatic C-H stretching. The results give an indication of the formation of an aromatic product. The peak around 2800-3000

cm⁻¹ is due to the stretching vibration of O-H present in water. UV/Vis data of lindane in hexane shows a prominent peak around 264 nm due to n – σ* transition as shown in Figure 2Ba. The decrease in the intensity of lindane peak suggests that lindane is getting removed from the solution after it reacted with RGO@Ag (Figure 2Bb). The absorbance of the solution starts increasing at 220 nm and continues into the deep UV region (below 200 nm). HRTEM image of RGO@Ag was taken after reacting with lindane and is shown in Figure 2C. The morphology of the composite does not change even after reacting with lindane. The HRTEM-EDAX of RGO@Ag after reaction shows the presence of chlorine (Figure 2D). The elemental mapping of the TEM image in Figure 2D also shows that chlorine is present only on silver. The spot SEM-EDAX of the composite shows the presence of silver along with chlorine (Figure S3). It is also evident from the elemental mapping in SEM image that there is a one-to-one correspondence with silver and chlorine. In other words, the presence of chlorine is prominent on the surface of silver, which supports the participation of Ag NPs in the degradation of lindane.

Lindane was also characterized using GC-ECD. A peak appeared at a retention time of 22 min for lindane and the solvent peak appeared around 2-3 min (as shown in Figure S4). The occurrence of new peaks (5-7 min) and decrease in lindane peak after the reaction indicate the formation of a new molecular species in the reaction media. Further conformation comes from the fact that GC-MS of lindane shows it's molecular ion at m/z 292 (Figure S5A) with isotope distribution for six chlorines, the spectrum matches with that in the literature. [*J. Microb.* 2008, 48, 134

The newly formed species has a molecular ion peak around m/z 180. This can be attributed to the formation of trichlorobenzene (TCB). The isotope pattern with peaks at m/z 181, 183 and 185 is due to the presence of three chlorines in TCB. There is no peak corresponding to m/z 292 (see Figure S5B), indicating the complete degradation of lindane to TCB. The spectrum of GC shows three distinct peaks for the products. The MS of these three peaks are almost similar, indicating the existence of TCB isomers in the product. The product was further confirmed using mass spectrometry (ESI-MS) as it is one of the best tools to precisely characterize any molecule. Lindane has a set of peaks in the range of m/z 292 (Figure 3A), corresponding to its molecular ion (in positive mode of ESI). The inset in the figure shows isotope distribution due to chlorine in the molecular ion. The degraded product of lindane was

also analyzed by MS (Figure 3B), a set of peaks arising around m/z 180 corresponds to an aromatic benzene ring with three chlorines (in the positive mode). Inset shows the enlarged spectrum in the region of m/z 180 where the isotope distribution for three chlorine atoms can be seen. The calculated spectrum matches perfectly with the experimental data. Probable structure of the product is shown in the inset which corresponds o trichlorobenzene (TCB). In order to establish the identity of the product, detailed tandem mass spectrometric (MS^2) studies were undertaken. MS^2 analyses of peaks at m/z 180, 182, 184 (corresponding to distinct isotopomers of the product) conducted at collision energy of 20 (in the instrumental unit) show the predicted isotope patterns as shown in Figure 4. This distinct fragmentation pattern confirms that the product is TCB. The MS^2 of m/z 179, 181 and 183 are shown in Figure 4(a-c). The peaks at m/z 179, 181, and 183 in the product are due to $^{35}Cl_3$,$^{35}Cl_2$, ^{37}Cl and ^{35}Cl, $^{37}Cl_2$ isotopomers of TCBs (of various isomers), respectively. The MS^2 of m/z 179 peak (Figure 4B, trace a) gives fragments at m/z 163, 151 and 136. The peak at m/z 163 is due to an exchange of one Cl by OH group, from the parent, m/z 179. The peak arising at m/z 151 is due to $C_6 H_9 Cl_{2+}$. Here, ^{35}Cl is lost in fragmentation. In the MS^2 of m/z 181, all the peaks are shifted by two mass units (trace b in Figure 4) higher than in trace a. Two peaks are seen at m/z 153 and 155 for the MS^2 of m/z 183 (trace c in Figure 4). Here there is a possibility of losing either ^{35}Cl or ^{37}Cl from the parent material. The enlarged full range MS^2 with higher collision energy (collision energy 60) is shown in Figure S6.

The reaction was carried out in large scale and the product was collected for further analysis. 100 mL of RGO@Ag was taken and 1 mL of lindane stock solution (5000 ppm) was spiked to it. The reaction was carried out for 1 h with continuous stirring. The product was phase transferred to hexane and kept for crystallization for a day. Needle-like crystals were formed (Figure 5B(i), insets). These crystals were characterized extensively. ^1H NMR of lindane (in CDCl 3), given in Figure 5A shows the characteristic peak at 4.64 ppm due to the presence of chemically equivalent six C-H bonds. The small peak at 7.26 ppm is due to $CDCl_3$, used as the solvent. Figure 5B shows the ^1H NMR spectrum of the product, the peaks between 7.2-7.5 ppm confirm the presence of aromatic hydrogen. Multiple peaks in the region confirm that mixtures of TCBs are formed in the reaction. Different isomers of TCB are shown in Figure 5A (inset). A small peak is visible around 4.63 ppm, due to the presence of un-reacted lindane, which got

attached to the crystals when all the material was dissolved in CDCl$_3$. The Raman spectrum of lindane in the inset of the Figure 5A (Figure 5A(a)) shows peaks at 500, 1510 and 1550 cm^{-1}, respectively due to C-Cl, and aliphatic C-C stretching modes. In the Raman spectrum of TCBs in the inset of Figure 5B (Figure 5B(b)), a peak at 430 cm^{-1} can be seen which confirms the presence of aromatic C-Cl stretching (the image shown here in Figure 5B(b) is after baseline correction). The original spectrum has large fluorescence background due to the conjugated double bond (shown in SI Figure S7).

Blank tests were performed to check the reactivity of graphene and Ag NPs separately, with lindane. We prepared 50 nm sized citrate capped Ag NPs (details of preparation and characterization are given in SI S8). We found that Ag NPs do not react with lindane even when kept for 6 h in contact. Similarly, RGO was also not having any affinity towards lindane. UV/Vis spectrum in Figure SI S9 (A and B) shows the adsorption/degradation capacity of Ag NPs and graphene separately, which was negligible for each case. Reactivity of lindane towards elemental silver was checked and it was found that elemental silver was indeed degrading lindane. However, the capacity of degradation was higher in the case of the composite (of about 100 times) when equal amount of silver was considered (Figure SI S10).

The composite (RGO@Ag) shows an unusual dehalogenation of lindane to various isomers of TCBs. The product, TCBs are also toxic in nature. So there is a need to find a suitable pathway for removal of these products from water. For this purpose, RGO@Ag was taken and lindane (dissolved in ethanol) was spiked, such that final concentration of lindane in the solution was 2 mg/L (ratio of water:ethanol was 500:1 (v/v)). Ethanol and water being completely miscible, there is no phase separation. In this case, graphene does not phase separate but remains dispersed in the solution, unlike in the previous case, when hexane was added. Hence, the composite gets adequate time to interact with the products formed. Characterization was done using GC-ECD and UV/Vis at different time intervals to monitor the change in concentration of lindane and TCBs in water. Initially lindane was showing a peak around the retention time of 22 min and the solvent appeared at 3-4 min in GC-ECD (Figure 6A). It was seen that with increase in contact time, the lindane peak started to disappear, ensuring its degradation. The peaks of TCBs started to appear around the retention time of 5-7 min. When the solution was stirred for 15 min, both the peaks for the degraded products (the isomers of TCBs) and of lindane

12

disappeared. Enlarged GC-ECD traces are given in Figure S11, so that these changes can be appreciated. The UV/Vis spectrum in Figure 6B also shows that at first lindane is degraded to TCBs and then both the peaks of lindane and TCBs disappeared. This suggests the removal of both lindane and TCBs from the solution. The removal capacity of lindane by the composite was found to be 99.90 % (for 2 ppm of lindane) by GC-ECD data.

It is known that silver has great affinity towards halogenated compounds. [*Langmuir* 2012, 28, 2671, 56] RGO react with lindane to form TCBs. This reaction is energetically favorable as the product gains aromaticity but further degradation of aromatic compounds is unlikely to be thermodynamically favorable, because of the high resonance energy of benzene ring (calculated value 152 kJ/mol). Graphene, the most promising adsorbent in the recent days was incapable of removing lindane from the solution when treated alone (SI Figure S9B), but was able to remove TCBs from the solution. This proposes a possible mechanism of adsorption onto graphene substrate. For conjugated organic molecules, it is physical adsorption which dominates and is likely to occur via π-π interaction. A mechanistic pathway showing the degradation of lindane followed by adsorption of the degraded product onto RGO@Ag is shown as schematic in Figure 7. The figure suggested that when lindane is spiked on RGO@Ag, Ag NPs reacts with lindane to form different isomers of TCBs. Silver on the graphene substrate changes to AgCl and remains attached on the graphene sheet. The TCB formed gets adsorbed on graphene sheet by π-π interactions. Thus it is seen that removal of lindane from water is a two-step process on RGO@Ag substrate. To confirm adsorption, the TCBs were extracted with a suitable eluent like hexane. 2 mL of hexane was added to the composite (after the reaction) and stirred vigorously for 10 min. The TCBs leave the graphene sheets and dissolve in hexane and the solution was characterized with GC-ECD, which shows peaks at a retention time of 5-7 min, characteristic of TCBs.

The reaction was evaluated under various conditions to check the viability of the material for practical applications. Increase in silver ion concentration during the preparation of RGO@Ag increases the size of Ag NP. However, the size of Ag NP in the window investigated does not affect the degradation efficiency of lindane (SI Figure S12). The removal capacity of RGO@Ag increases with dilution, probably due to the increase in free surface area available upon dilution (Figure 8A). The maximum removal capacity for lindane was found to be 827

mg/g of the composite. Effect of pH towards removal capacity was checked and it was seen that pH does not have any affect in the window of 3-9 (Figure 8B). But capacity decreases with pH higher than 9, because of the formation of silver hydroxide, thus decreasing the free silver sites available for degradation of lindane. The reaction was also performed in TW for real time application. It shows removal capacity to be 80 % as compared to laboratory batch experiments (SI Figure S13A). The removal capacity of the composite was checked for common ion effect. For this, 5 ml of RGO@Ag was taken and NaCl solution was spiked to it such that the final concentration of the solution was 100 ppm of Cl^-. The removal efficiency of composite was found to be 65 % as compared to the laboratory batch experiment (SI Figure S13B).

Conclusion: In summary, the presentor report an unusually efficient dehalogenation reaction on graphene-silver nanocomposites. The conversion of an alycyclic compound, lindane to trichlorobenzene is reported for the first time on a graphene substrate. In the reaction, lindane was dehydrohalogenated to yield different isomers of trichlorobenzene and then the products were adsorbed on graphene substrate by π-π interactions. By this process, a persistent organopesticide was effectively removed from water at an efficiency close to 99.90 %. High adsorption capacity of lindane, 827 mg/g, on the composite, can be effectively used for decontaminating water. This type of reaction can be employed for the degradation of other toxic halocarbons which may open up a new method for environmental remediation.

It may be appreciated by those skilled in the art that the drawings, examples and detailed description herein are to be regarded in an illustrative rather than a restrictive manner.
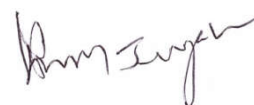
We Claim:

1. A method of removing lindane from water at an efficiency of 99.90% in a time span of 15 min using a graphene-metal nanocomposite by dehydrohalogenating lindane to different isomers of trichlorobenzene (TCB) and simultaneously adsorbing the dehydrohalogenated product wherein the said method comprises

     a. reaction of the metal nanoparticles in the composite with lindane to form different isomers of trichlorobenzene (TCB) and

     b. adsorption of the trichlorobenzene (TCB) on to a graphene sheet.

2. The method as claimed in claim 1, wherein the metal is a silver nanoparticle (AgNp) of size ranges from 5-50 nm.

3. The method as claimed in claim 1, wherein adsorption of trichlorobenzene (TCB) on to the graphene sheet is by π-π interactions.

4. The method as claimed in claim 1, wherein the degradation of lindane to isomers of TCB by silver nanoparticle (AgNp) and adsorption of the degraded product on to graphene sheets occurs simultaneously.

5. The method as claimed in claim 1, wherein the method is efficient in the pH range of 4-9

6. The method as claimed in claim 1, wherein adsorption of lindane is 827 mg/g of the nanocomposite.
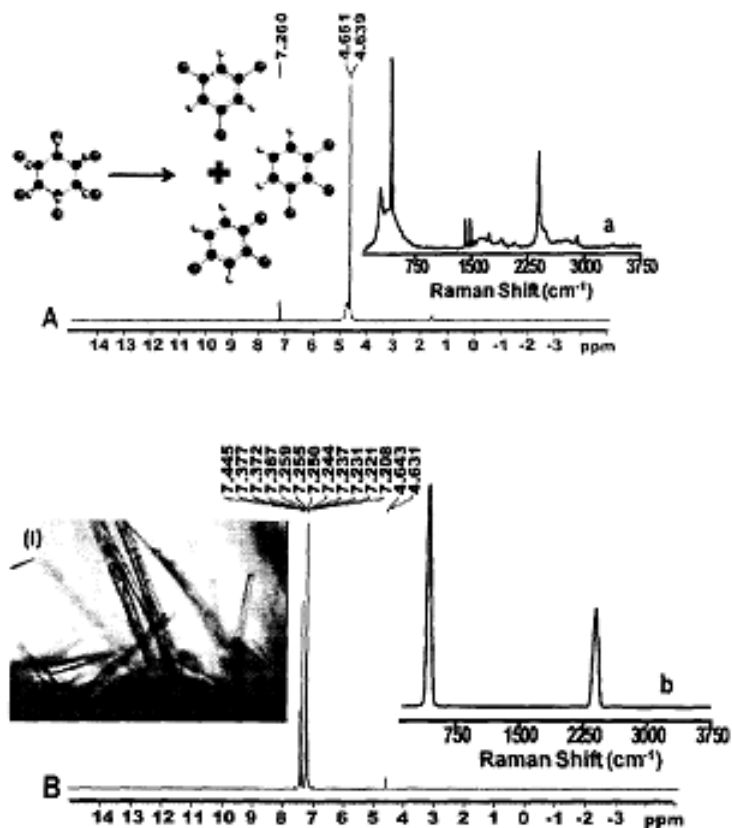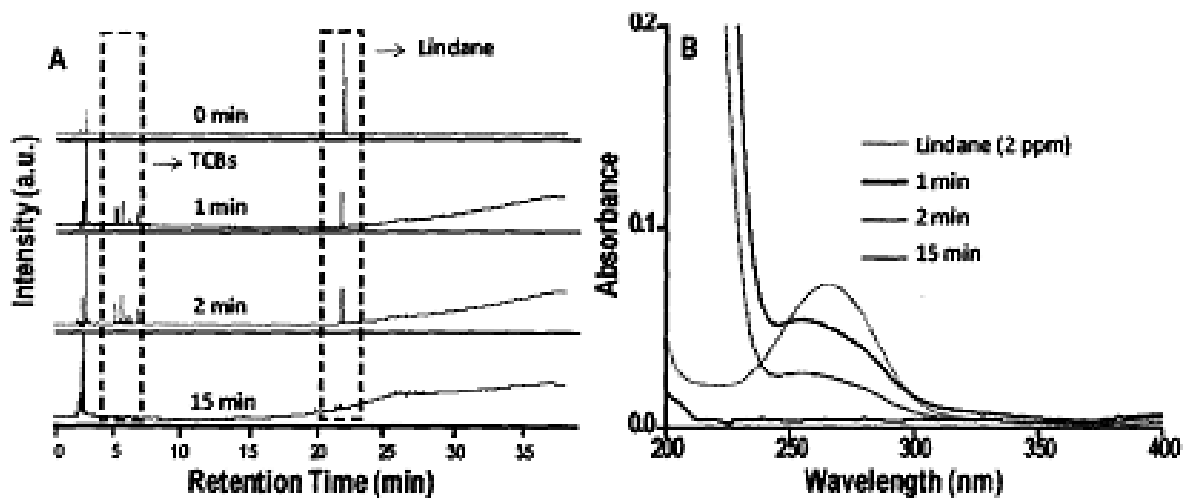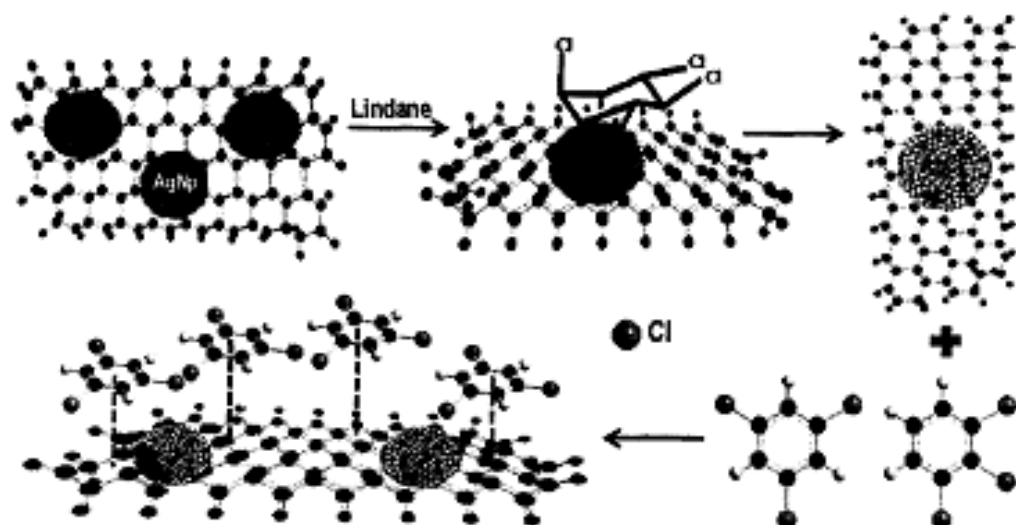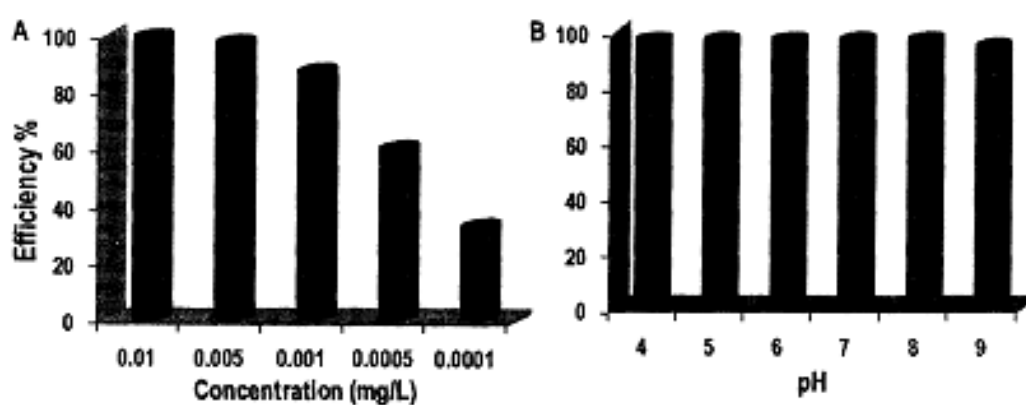

Dated at Chennai this 07 September, 2018

Signature:

   D. Moses Jeyakaran
   Advocate & Patent Agent
   IN/PA - 369

METHOD OF REMOVING LINDANE FROM WATER BY GRAPHENE-METAL NANOCOMPOSITE

ABSTRACT

The present invention relates to a method of removing lindane from water using a graphene nanocomposite by degradation of lindane to different isomers of trichlorobenzene (TCB) over a silver nanoparticle supported on reduced graphene oxide (RGO).

METHOD OF REMOVING LINDANE FROM WATER BY GRAPHENE-METAL NANOCOMPOSITE

APPLICATION NUMBER: 5988/CHE/2013
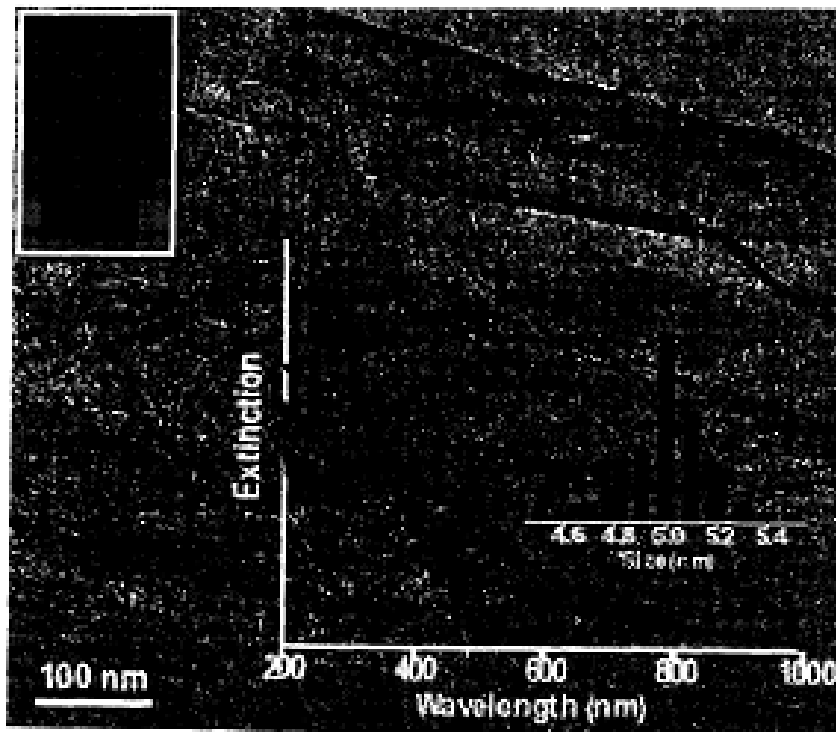
Figure 1

Signature:

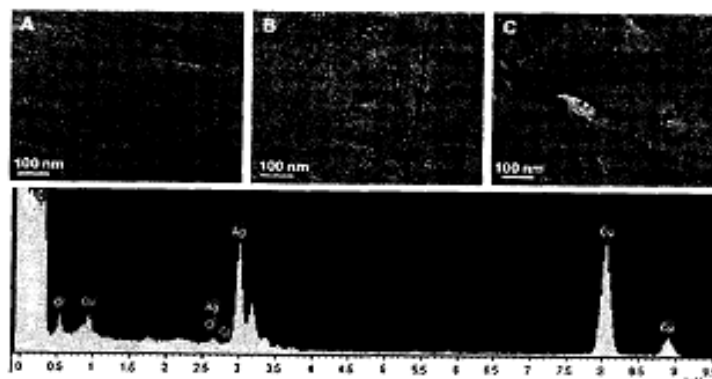D. Moses Jeyakaran
Advocate & Patent Agent
IN/PA — 369

METHOD OF REMOVING LINDANE FROM WATER BY GRAPHENE-METAL NANOCOMPOSITE

APPLICATION NUMBER: 5988/CHE/2013
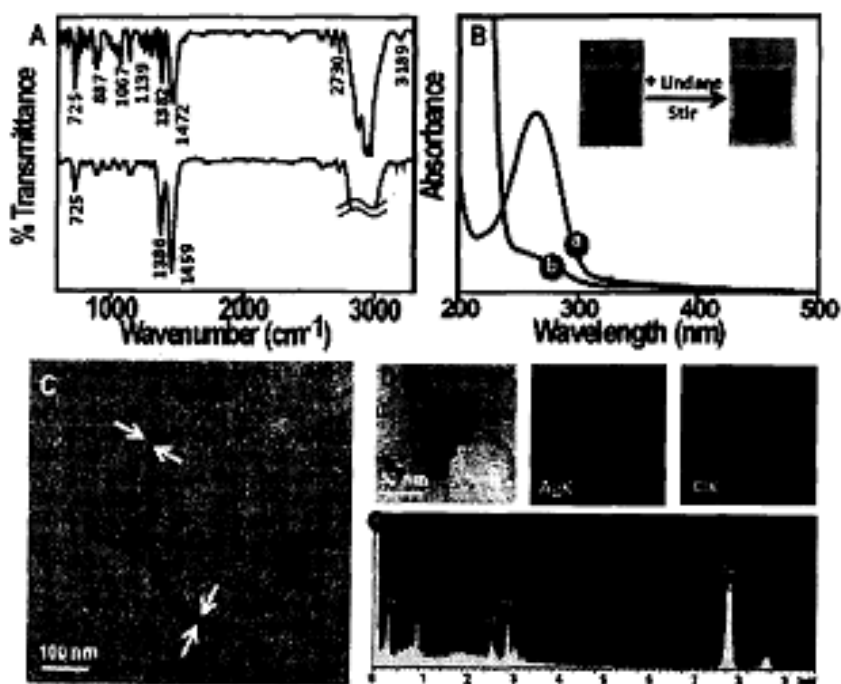
Figure 2

Signature:

D. Moses Jeyakaran
Advocate & Patent Agent
IN/PA — 369

METHOD OF REMOVING LINDANE FROM WATER BY GRAPHENE-METAL NANOCOMPOSITE

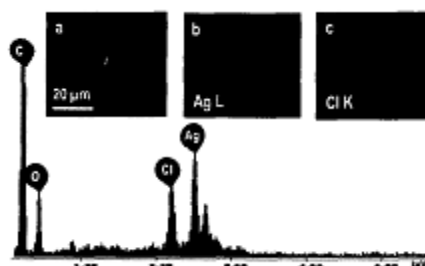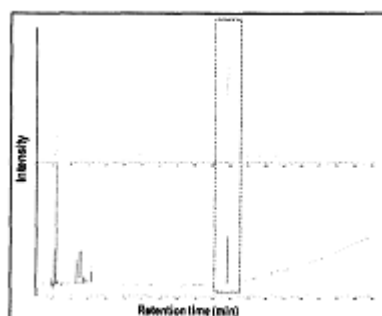APPLICATION NUMBER: 5988/CHE/2013
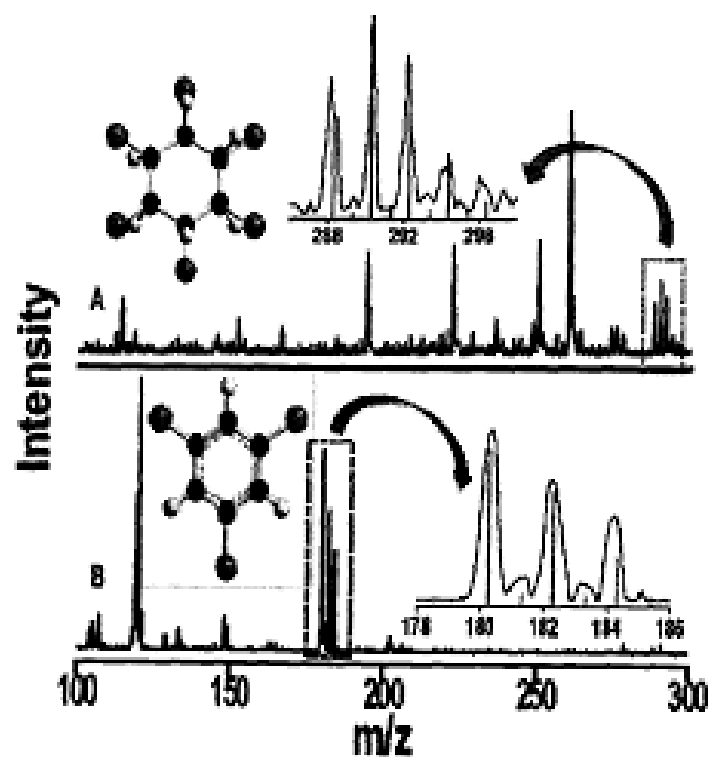
Figure 3

Signature:

D. Moses Jeyakaran
Advocate & Patent Agent
IN/PA — 369

METHOD OF REMOVING LINDANE FROM WATER BY GRAPHENE-METAL NANOCOMPOSITE

APPLICATION NUMBER: 5988/CHE/2013
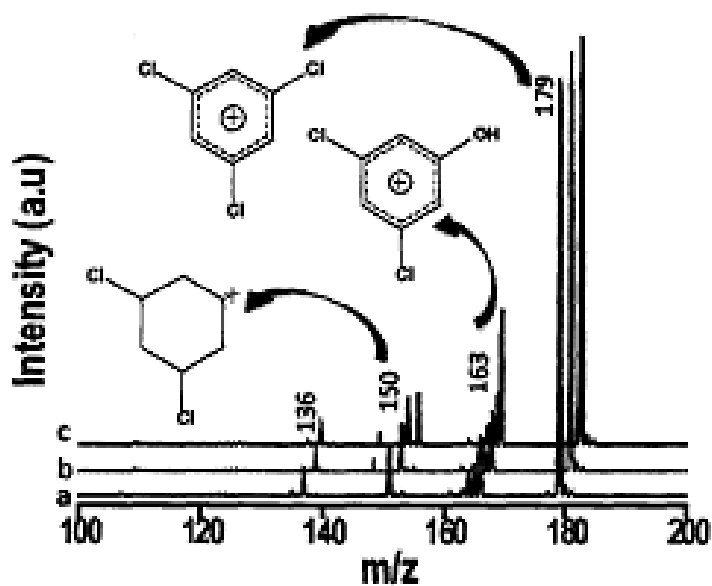
Figure 4

Signature:

D. Moses Jeyakaran
Advocate & Patent Agent
IN/PA — 369

METHOD OF REMOVING LINDANE FROM WATER BY GRAPHENE-METAL NANOCOMPOSITE

APPLICATION NUMBER: 5988/CHE/2013
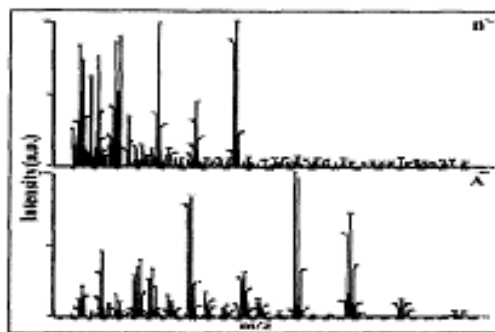

Figure 5

Signature:

D. Moses Jeyakaran
Advocate & Patent Agent
IN/PA — 369

METHOD OF REMOVING LINDANE FROM WATER BY GRAPHENE-METAL NANOCOMPOSITE

APPLICATION NUMBER: 5988/CHE/2013
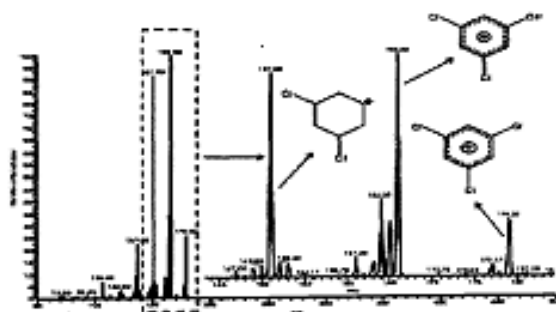

Figure 6

Signature:

D. Moses Jeyakaran
Advocate & Patent Agent
IN/PA — 369

METHOD OF REMOVING LINDANE FROM WATER BY GRAPHENE-METAL NANOCOMPOSITE

APPLICATION NUMBER: 5988/CHE/2013

Figure 7

Signature:

D. Moses Jeyakaran
Advocate & Patent Agent
IN/PA — 369

METHOD OF REMOVING LINDANE FROM WATER BY GRAPHENE-METAL NANOCOMPOSITE
APPLICATION NUMBER: 5988/CHE/2013

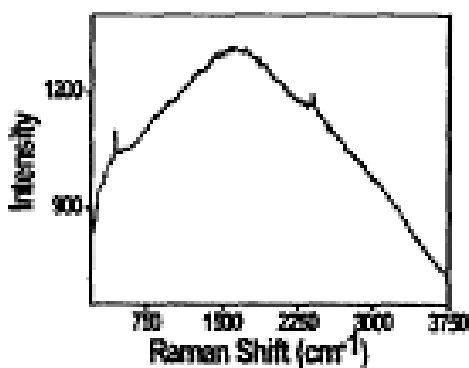
Figure 8

Signature:

D. Moses Jeyakaran
Advocate & Patent Agent
IN/PA — 369

METHOD OF REMOVING LINDANE FROM WATER BY GRAPHENE-METAL NANOCOMPOSITE
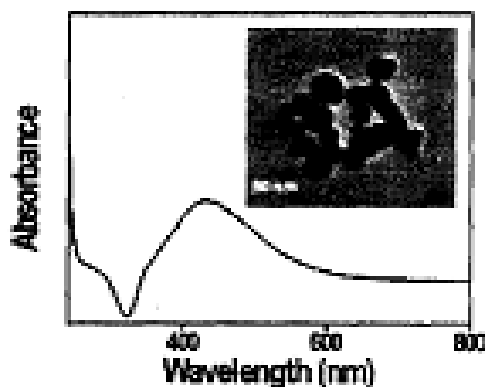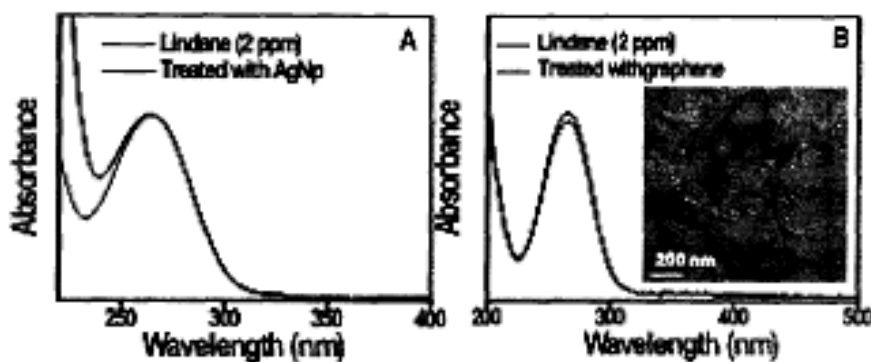APPLICATION NUMBER: 5988/CHE/2013

Figure S1

Figure S2

Signature:

D. Moses Jeyakaran
Advocate & Patent Agent
IN/PA — 369

METHOD OF REMOVING LINDANE FROM WATER BY GRAPHENE-METAL NANOCOMPOSITE

Figure S3

Figure S4

Signature:

D. Moses Jeyakaran
Advocate & Patent Agent
IN/PA — 369

METHOD OF REMOVING LINDANE FROM WATER BY GRAPHENE-METAL NANOCOMPOSITE
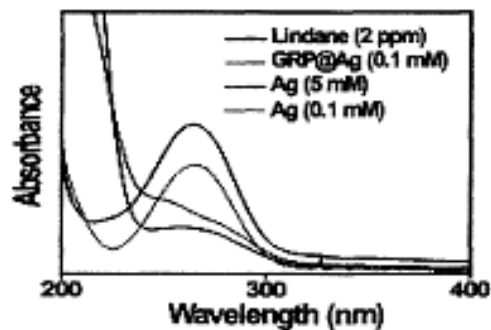APPLICATION NUMBER: 5988/CHE/2013

Figure S5

Figure S6

Signature:

D. Moses Jeyakaran
Advocate & Patent Agent
IN/PA — 369

METHOD OF REMOVING LINDANE FROM WATER BY GRAPHENE-METAL NANOCOMPOSITE

APPLICATION NUMBER: 5988/CHE/2013

Figure S7

Figure S8

Figure S9

Signature:

D. Moses Jeyakaran
Advocate & Patent Agent
IN/PA — 369

METHOD OF REMOVING LINDANE FROM WATER BY GRAPHENE-METAL NANOCOMPOSITE
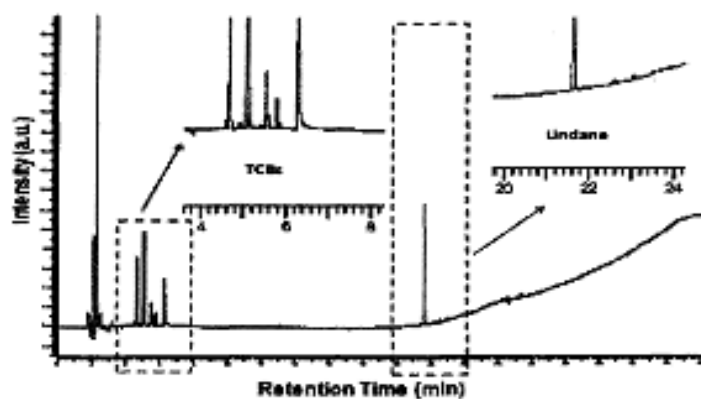APPLICATION NUMBER: 5988/CHE/2013

Figure S10

Figure S11

Signature:

D. Moses Jeyakaran
Advocate & Patent Agent
IN/PA — 369

METHOD OF REMOVING LINDANE FROM WATER BY GRAPHENE-METAL NANOCOMPOSITE
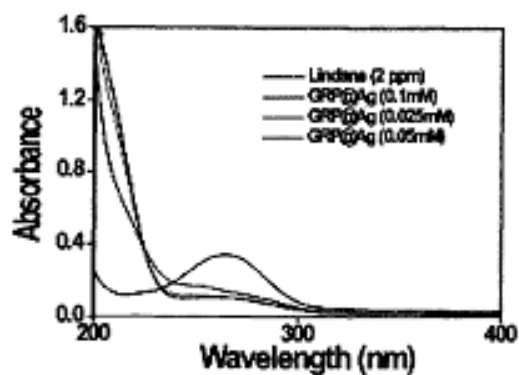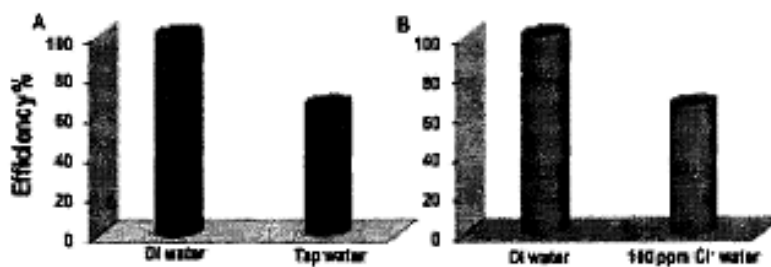
APPLICATION NUMBER: 5988/CHE/2013

Figure S12

Figure S13

Signature:

D. Moses Jeyakaran
Advocate & Patent Agent
IN/PA — 369